https://doi.org/10.3311/PPch.44877
Creative Commons Attribution

Periodica Polytechnica Chemical Engineering

Modified Lignins from Electrochemical Treatment of Black Liquor and their Characterization

Himadri Roy Ghatak[1*]

[1] Department of Chemical Engineering, Sant Longowal Institute of Engineering and Technology, 148106 Longowal, Punjab, India
[*] Corresponding author, e-mail: hrghatak@sliet.ac.in

Received: 26 May 2026, Accepted: 24 September 2026, Published online: 18 November 2026

Abstract

Black liquor (BL) obtained from wheat straw by the soda process was electrochemically treated to different specific charge (SC) at different current densities (CD). Lignins were acid precipitated from the treated BL and characterized for yield (gravimetrically), phenolic hydroxyl (Folin and Ciocalteu method), molecular structure (NMR spectroscopy), and thermal stability (thermogravimetry). Lignin obtained from untreated BL was the control for comparison. Process yielded lesser lignin when the BL was electrochemically treated at lower CD and higher SC. Lignins obtained after electrochemical treatment of BL had appreciably higher phenolic hydroxyl content: 18.9 to 48.9% increase over control. Compared to 0.89 ± 0.01 mmol/g in the control, the highest phenolic hydroxyl content of 1.34 ± 0.02 mmol/g was obtained by electrochemically treated BL at 5.55 ± 0.01 mA/cm^2 CD and SC of 0.115 ± 0.001 A·h/g organic content in BL. Methoxyl content in the lignin macromolecule and the relative abundance of syringyl also underwent appreciable decrease by BL electrochemical treatment. The control lignin had 118.3 methoxyl groups per 100 phenylpropane, and a syringyl/guaiacyl ratio of 0.41. These values reduced to 94.6, and 0.04, respectively, at 5.55 ± 0.01 mA/cm^2 CD and SC of 0.46 ± 0.005 A·h/g organic content in BL. Electrochemical soda lignins were thermally more stable than soda lignin up to 625 °C.

Keywords

electrochemical treatment, lignin, S/G ratio, phenolic hydroxyl, thermal stability

1 Introduction

In the backdrop of the quest for sustainable development, the vegetative component lignin is of particular importance. The availability of lignin is conservatively estimated to be in excess of 300 billion tons [1]. However, this abundant renewable material remains grossly underutilized. It can substitute petroleum derived materials in the aromatic domain if its potential is fully harnessed. Therefore, value addition to lignin remains one of the primary challenges to the widespread success of lignocellulosic biorefineries [2]. The industrial process to convert lignocellulose into papermaking and dissolving grade pulp yields a lignin rich byproduct stream, the black liquor (BL). Alkaline pulping, primarily kraft and to a lesser extent soda, is the predominant method to convert lignocellulose into pulp. It is customary to burn the lignin present in the BL for captive energy generation. However, studies reveal that it should be possible to put a substantial part of this lignin to non-energy applications without jeopardizing the energy needs of pulping operations [3].

There have been numerous attempts to use alkali lignin as the starting material for the synthesis of polymers [4–6], carbon materials [7–9], and low molecular weight aromatics [10–12]. Among the various constraints to adding value to lignin, its chemical heterogeneity remains a major challenge. This heterogeneity can arise from the difference in lignocellulose source material as well as from the method of lignin isolation [2]. Lignin macromolecule is made up of phenylpropane monomer constituent units. These units are varied in terms of the functional groups present on the aromatic ring and the aliphatic side chain. Moreover, the linkages joining these monomer units and their combinations also vary. Based on the starting lignocellulose and the isolation method, the lignin characteristics may vary. This is particularly notable for the number and positioning of methoxyl groups on the aromatic ring [13–15]. Similarly, the content of phenolic hydroxyl and aliphatic hydroxyl groups differ in lignins obtained from different lignocelluloses using

Cite this article as: Roy Ghatak, H. "Modified Lignins from Electrochemical Treatment of Black Liquor and their Characterization", Periodica Polytechnica Chemical Engineering, 2026. https://doi.org/10.3311/PPch.44877

different isolation protocols [14, 16]. Equally diverse is the relative abundance of different intermonomer linkages and substructural moieties in lignins obtained from different sources [14, 15, 17]. Therefore, it is highly desirable to characterize lignin after its isolation from the lignocellulose and before its intended end use.

Chemical modification of alkali lignin – soda or kraft – is one of the several methods to tailor its characteristics for particular application. One possible route for lignin derivatization is hydroxymethylation where lignin dissolved in aqueous alkali is reacted with formaldehyde [18, 19]. In a variation, reaction of lignin solution in aqueous alkali was effected with amines to get aminated lignin [20]. Similarly, lignin can be glyoxalated through reaction with glyoxal in alkaline medium [18]. The methyl moiety in the methoxyl groups was substituted with hydrogen. This increased the phenolic hydroxyl content of lignin. Lignin dissolved in aqueous alkali was heated in the presence of sodium sulphite for this purpose [21]. There are reports of carboxymethylation of lignin by reaction with sodium chloroacetate in the presence of sodium hydroxide [22]. In all these modification protocols lignin was first obtained from acidification of BL. It was then redissolved in aqueous alkali and modified with the addition of the designated chemical agent. After the reaction, the modified and/or derivatized lignin is to be reprecipitated from the alkaline solution. This would effectively require six process steps – acidification of BL, filtration and washing of precipitated lignin, redissolution of lignin in aqueous alkali, chemical modification of lignin, acid precipitation of modified lignin, and filtration and washing of precipitated modified lignin.

Number and positioning of methoxyl groups on the aromatic ring as well as the phenolic hydroxyl content are important lignin characteristics for its intended value added use. Early studies have revealed that lignin reacts during phenol formaldehyde (PF) resin synthesis through its unsubstituted ortho position relative to the phenolic hydroxyl [23]. Decrease in methoxyl groups abundance and increase in phenolic hydroxyl content in lignin was found to increase lignin reactivity during synthesis of PF resin [21, 24]. Abundance of phenolic hydroxyl groups are important because urethane linkages are formed by the reaction of hydroxyl group of the polyol with the isocyanate group when lignin is used as a polyol substitute in polyurethane synthesis [25, 26]. It is also reported that phenolic hydroxyl groups are more reactive to the formation of urethane linkages in the order p-hydroxyphenyl (H) > guaiacyl (G) > syringyl (S) [27]. Lignin is often oxypropylated prior to its use in polyurethane synthesis. It was observed that higher abundance of phenolic hydroxyl facilitates lignin oxypropylation [28]. Carboxymethylation, another important modification to increase its hydrophilic character, proceeds through the reaction between the phenolic hydroxyl of lignin and chloroacetate [22]. Epoxidation of lignin is also known to proceed through its phenolic hydroxyl functionality [29, 30]. The prepared resin is more crosslinked with improved thermomechanical properties if the lignin is preferentially of G type [31].

Besides lignin applications in resin synthesis, its another value added application could be in polymer composites and blends. Due to its aromatic nature, lignin leaves a larger amount of char residue upon thermochemical degradation. This characteristic combined with its relatively slower rate of thermal degradation could enhance the thermal stability and/or fire retardant properties of polymer composites and blends [2]. Incorporation of calcium lignosulphonate improved thermal stability and fire retardant characteristics of phenolic foam [6]. Use of softwood, hardwood, and bagasse kraft lignins as polyol substitute for synthesizing polyurethane foam improved the thermal stabilities of the resulting products [5]. Blending enzyme hydrolysis lignin with epoxy resin increased the limiting oxygen index and decreased heat release and smoke, an indication of improved flame retardance [4].

Electrochemical oxidation of lignin is an upcoming method to convert alkali lignin into valuable low molecular weight oxygenated aromatic compounds like vanillin, acetovanillone, syringaldehyde, and acetosyringone. Elecxtrochemical methods have an inherent advantage as electrolyzers are modular by design and can be stacked into batteries to scale up the process. Lignin degradation on stainless steel (SS) anode followed a pseudo first order kinetics during the electrochemical oxidation of wheat straw and bagasse soda lignins in aqueous alkaline solution. Overall, the process was found to be a multiple reaction combining series and parallel reactions. The vanillin concentration attained a maximum for a given specific charge (SC) [11]. In a related study, electrochemical oxidation on SS and Titanium-mixed metal oxide anodes of wheat straw and bagasse soda lignins in aqueous alkaline solution produced the aromatic carbonyl compounds vanillin, syringaldehyde, acetosyringone, apocynin, and benzaldehyde. The yields were dependent on current density (CD) and SC [12, 32]. Electrochemical oxidation of softwood lignin in aqueous alkaline solution produced vanillin that could be separated from the reaction mixture

by adsorption [33]. In another study, the cathode and anode chambers were separated by anion exchange membrane. Aqueous alkaline solution of kraft lignin flowed through the anode chamber while the cathode chamber contained NaOH solution. Nickel electrodes of different morphologies were used. Major reaction products were separated by ultrafiltration and identified as guaiacol, coniferyl alcohol, vanillin, syringaldehyde, and apocynin. Ultrafiltration retentate containing unreacted lignin was returned to the electrochemical reactor [34]. These electrochemical modification methods were also applied to lignin previously obtained from acidification of BL after redissolving it in aqueous alkali, therefore, requiring six process steps. Moreover, the lignin not converted to target low molecular weight compounds was left unattended and uncharacterized. In the present work soda BL from wheat straw was directly subjected to electrochemical treatment (ET) at controlled process conditions. After ET the undegraded lignin was acid precipitated from the BL and characterized for its modified properties. In effect, the process can be carried out in three steps – ET of BL, acid precipitation of modified lignin, and filtration and washing of precipitated modified lignin. Combined with the possibility of producing valuable low molecular weight aromatic compounds alongside a modified lignin, the proposed approach can provide the pulp mills with a simpler alternative process layout to lignin value addition.

2 Materials and methods

2.1 Materials

Wheat straw soda BL used in the study was obtained from a nearby paper mill and filtered through 200 mesh screen to separate any suspended particles. The BL was stored under refrigeration at 4 °C. It was analyzed for dissolved solids concentration, pH and organic and inorganic content of dissolved solids according to TAPPI standard method T-650 pm-84 [11]. The main BL characteristics are shown in Table 1.

Reagents used in the study were of analytical grade and procured from S D Fine-chem Ltd., Mumbai, India. Whenever required, deionized water was sourced from the laboratory Millipore (USA) RiOS 5 Century Synergy water purification system. 1 mm thick SS 304 sheet conforming to IS 6911:2017 standard [35] was procured from the vendor in the local market for electrode material.

Table 1 Main BL characteristics

BL characteristics	Value
Dissolved solids	9.80 ± 0.01%
Organics in dissolved solids	63.3 ± 0.5%
Inorganics in dissolved solids	36.7 ± 0.5%
Organic/inorganic ratio	1.72
pH	11.51 ± 0.02

2.2 Electrochemical treatment of black liquor

Each electrochemical run was performed with 200 mL BL in a beaker. Prior to ET, the BL was allowed to reach the prevailing temperature in the laboratory, which was maintained at 25 ± 1 °C. All ET experiments were carried out at this condition. Electrodes with 90 cm^2 working area were placed in the BL at 5 mm inter-electrode gap. Galvanostatic conditions were maintained with a Tonghui (China) TH6402A Programmable DC power supply. It was observed that electrolytic gases evolved at both cathode and anode during ET which kept the BL well mixed. Each ET experiment was performed twice. At the end of the electrochemical run, the treated BL was filtered to remove any suspended impurity. The filtered BL was acidified by addition of 0.5 mol/L HCl to an end pH 2. This caused the lignin to precipitate. The acidified mass was placed for 1 h at 75 °C in a hot air oven followed by filtration. Filtered lignin was washed with deionized water till the washings were neutral. Washed lignin was dried in hot air oven at 105 °C and weighed for yield. It was subsequently used for further analyses. Soda lignin (SL) was similarly obtained from untreated BL by acidification, filtration, and washing. The ET conditions used, and the labels for the resulting lignins are described in Table 2.

Inter-electrode potential was 3.05 ± 0.02 V during ET for electrochemical soda lignins ESL1 and ESL2. The inter-electrode potential was 2.42 ± 0.01 V during ET for ESL3 and ESL4. SC was calculated as:

$$\mathrm{SC} = \frac{I \cdot t}{m \cdot C \cdot O}, \tag{1}$$

where I is the current in A, t is the time in h, m is the mass of BL, C is the mass fraction of dissolved solids in BL and O is the mass fraction of organics of dissolved solids in BL.

Table 2 Electrochemical treatment conditions with associated standard deviation (SD) in bracket and the resulting lignin labels

Lignin label		CD (mA/cm^2)	SC (A · h/g organics in BL)
Soda lignin (SL)		0	0
Electrochemical soda lignin	ESL1	11.11 ± 0.02 (0.03)	0.115 ± 0.001 (0.001)
	ESL2	11.11 ± 0.02 (0.03)	0.46 ± 0.005 (0.007)
	ESL3	5.55 ± 0.01 (0.01)	0.115 ± 0.001 (0.001)
	ESL4	5.55 ± 0.01 (0.01)	0.46 ± 0.005 (0.007)

2.3 Lignin characterization

2.3.1 Phenolic hydroxyl content

Phenolic hydroxyl content in lignin was determined by the Folin and Ciocalteu method [16]. Vanillin, dissolved in dimethyl sulfoxide (DMSO) at 0.01–0.05 mM concentration, was used as the phenol calibration standard. The lignin was dissolved in DMSO at a concentration 1 g/L. The reaction mixture was prepared by the addition of 0.5 mL lignin solution, 1.5 mL Folin reagent, and 15 mL DMSO in a 25 mL volumetric flask. 5 mL of 200 g/L Na_2CO_3 was added to the reaction mixture after allowing it to stand for 10 min. The flask was filled to 25 mL with DMSO. The reaction was allowed to complete in 2 h with occasional shaking. A similar method was used for preparing the calibration curve by substituting vanillin solution for lignin in the reaction mixture. At the end of the reaction its absorbance was recorded at 760 nm using a Jenway (UK) Genova Bio UV-Vis spectrophotometer. Concentrations of phenolic hydroxyl in the lignin solutions were determined by correlating with the calibration obtained from the absorbances of vanillin solutions. Phenolic hydroxyl content in lignin was determined as follows:

$$\text{Phenolic hydroxyl}\left(\frac{\text{mmol}}{\text{g}}\right)=\frac{C_{\text{Phenolic OH}}}{C_{\text{Lignin}}}, \tag{2}$$

where $C_{\text{Phenolic OH}}$ is the concentration of phenolic hydroxyl in mM as determined by absorbance measurement, and C_{Lignin} is the concentration of lignin solution prepared in g/L.

2.3.2 NMR characterization

Solution-state NMR spectra were recorded by dissolving lignin in DMSO-D6 at 70 mg/mL concentration. The complete dissolution before NMR experiment was ensured by overnight stirring. The instrument used was Bruker (Germany) Avance Neo 500 MHz NMR spectrometer. Pulse sequences used were: for ^{1}H zg30, and for ^{1}H–^{13}C HSQC hsqcetgp. 64k data points were recorded for the ^{1}H spectra spanning over 128 scans. The relaxation delay was 1 s. The HSQC spectra were recorded with 2048, and 1024 data points in the ^{1}H (direct), and ^{13}C (indirect) dimensions, respectively. The experiment was run with 1.5 s relaxation delay, 8 acquisition scans per increpent, and 145 Hz ^{1}J coupling constant. The signal integrations were performed using MestReNova 6.0.2.5475 [36].

2.3.3 Thermochemical characterization

SL and ESLs were characterized by thermogravimetric analysis (TGA) in a Netzsch (Germany) TG 209 F3 Tarsus instrument. The specimens (10–12 mg) were heated in an alumina crucible in nitrogen atmosphere of 20 mL/min. The temperature ramp was 50 °C/min.

2.3.4 Ash determination

The ash content in the lignin samples were determined by placing a known mass (about 500 mg) of the sample in a tared silical crucible and keeping it in a muffle furnace at 900 °C for 4 h. Then the crucible was taken out from the furnace, cooled in a desiccator, and weighed. The crucible was again put in the furnace for another 1 h, taken out from the furnace, cooled in desiccator, and weighed. The procedure was repeated till constant mass is achieved. Measurements were made in duplicate.

3 Results and discussion

3.1 Gross lignin yield and ash content

The CD during the ET of BL has a profound effect on the lignin yield obtained after acidification. Untreated BL (solids concentration 9.80%) yielded gross amount of 45.86 g, lignin SL/L BL, which was 78% of the organics present in BL. This lignin had 2.82% ash in it. BL ET at 11.11 mA/cm^2 CD for SC 0.115 A·h SC/g organics in BL had negligible effect on gross lignin ESL1 yield. It had a ash content of 2.76% in it. When the ET at same CD was increased to SC 0.46 A·h/g organics in BL, the gross lignin ESL2 yield reduced to 42.02 g/L BL, a yield reduction of 8%. The ash content in this lignin was 3.11%. At reduced CD of 5.55 mA/cm^2, lignin ESL3 gross yield from electrochemically treated BL for SC 0.115 A·h/g organics in BL was 38.07 g/L BL. This lignin had ash content of 2.79%. At this CD, lignin ESL4 gross yield dropped to only 19.26 g/L BL when SC of ET was increased to 0.46 A·h/g organics in BL. The ash content in this lignin was 3.05%. This substantial drop of 58% in lignin yield clearly indicates extensive lignin degradation. Lignin degradation during ET in alkaline medium is well known and the present findings are in agreement with previous studies [11, 12]. However, it is interesting to note that higher CD cause less lignin degradation. The primary reason for the degradation of the organic compounds during ET is the formation of radical oxidant species $OH^{\bullet}$ (redox potential 2.8 V) according to the following reaction [37]:

$$H_2O \rightarrow OH^{\bullet} + e^{-} + H^{+}. \tag{3}$$

Along with the hydroxyl radicals, several other oxidant species like $O_2^{\bullet-}$ (redox potential 1.56 V), $O^{\bullet}$, and O_2 (redox potential 1.57 V) could also form as a result of different

reactions, as shown below [37–39]. (Here, all the redox potentials are reported *vs.* standard hydrogen electrode).

$$2OH^- \rightarrow O^\bullet + H_2O + 2e^- \quad (4)$$

$$OH^\bullet \rightarrow O^\bullet + e^- + H^+ \quad (5)$$

$$2OH^\bullet \rightarrow O^\bullet + H_2O \quad (6)$$

$$2O^\bullet \rightarrow O_2 \quad (7)$$

$$O_2 + e^- \rightarrow O_2^{\bullet -} \quad (8)$$

These species, especially O_2, are weaker oxidants than $OH^\bullet$ and react to a lesser extent with the organics present. Among other factors, the formation of oxidant species is strongly dependent on the potential at the electrode which is directly linked to the CD of ET. Higher CD with associated higher electrode potential favours the formation of secondary oxidant species over hydroxyl radical formation [37]. It is important to mention that the variation in the inter-electrode potential during each ET was less than 1% during the entire experimental run. It indicates that the electrode surface remained stable and free from any passivation at the applied CDs.

3.2 Phenolic hydroxyl content

SL has 0.89 mmol phenolic hydroxyl group/g lignin. ET of BL prior to the lignin isolation increases the content of phenolic hydroxyl groups in the resulting lignins. With ET at 11.11 mA/cm^2 CD for 0.115 A·h SC/g organics in BL, the produced ESL1 has 1.08 mmol phenolic hydroxyl group/g lignin – an increase of 20% over SL. With the SC increasing to 0.46 A·h/g organics in BL, ESL2 has 1.02 mmol phenolic hydroxyl groups per g lignin – increase of 13.3% over SL. BL ET at 5.55 mA/cm^2 CD for 0.115 Ah SC per g organics produced ESL3 with 1.34 mmol phenolic hydroxyl groups per g lignin – increase of 48.9% over SL. Finally, ET to 0.46 Ah SC per g organics in BL at 5.55 mA/cm^2 CD, resulted in ESL4 having 1.07 mmol phenolic hydroxyl groups per g lignin – increase of 18.9% over SL. One possible reason for the increased phenolic hydroxyl content in lignin after ET of BL could be the cleavage of aryl-alkyl ether linkages. For any SC, lower CD has an increasing effect on the lignin phenolic hydroxyl content. And, for lower CD, lower SC produces lignin with more phenolic hydroxyl. But the trend is reversed for higher CD. These lignins with increased phenolic hydroxyl content are likely to be more valuable in applications as sustainable phenol/polyphenol substitute for PF and epoxy resins and polyurethanes. A comparative account of lignin yield, ash, and phenolic hydroxyl content is presented in Table 3.

3.3 Qualitative ^{1}H–^{13}C HSQC NMR characterization

The ^{1}H–^{13}C HSQC NMR spectra of the SL is shown in Fig. 1. Enlarged version of Fig. 1 and spectra of the ESLs are shown in the Supplement (Figs. S1 to S5).

3.3.1 Methoxyl, and oxygenated aliphatic side chain

The attributed H–C correlations are tabulated in Table 4 [14, 17, 40–47]. There are three cross peaks associated with the different *β*–O–4′ linked moieties in the spectrum of SL. Entities with *β*–O–4′ along with *α*–O–4″ intermonomer linkages by

Table 3 Comparison of lignin yield and phenolic hydroxyl content at different ET conditions

Lignin sample	Gross yield (g/L BL)	Ash content (%)	Phenolic hydroxyl content (mmol/g lignin)
SL	45.86 ± 0.42 (0.59)	2.82 ± 0.08 (0.11)	0.89 ± 0.01 (0.01)
ESL1	45.81 ± 0.42 (0.59)	2.76 ± 0.07 (0.10)	1.08 ± 0.01 (0.01)
ESL2	42.02 ± 0.44 (0.62)	3.11 ± 0.10 (0.14)	1.02 ± 0.01 (0.001)
ESL3	38.07 ± 0.36 (0.51)	2.79 ± 0.08 (0.11)	1.34 ± 0.02 (0.003)
ESL4	19.26 ± 0.21 (0.30)	3.05 ± 0.09 (0.13)	1.07 ± 0.01 (0.01)

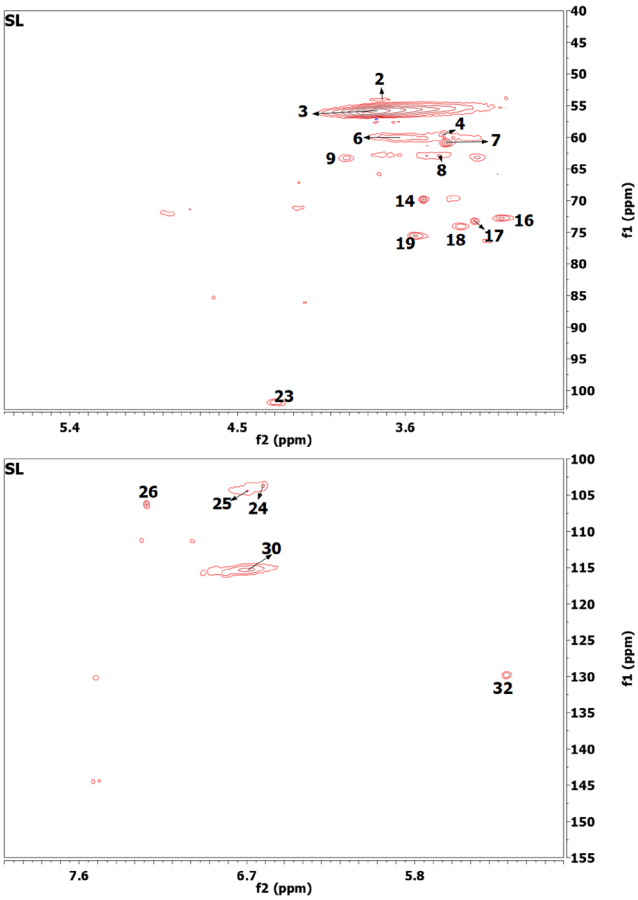


Fig. 1 ^{1}H–^{13}C HSQC NMR spectrum of SL

Table 4 $^{1}H–^{13}C$ HSQC NMR signal assignment of lignin molecular substructures and functionalities in the 2.75–5.75/40–105 ppm regions [14, 17, 40–47]

Signal identity in spectrum	Assignment	Presence of peaks				
		SL	ESL1	ESL2	ESL3	ESL4
1	Cα–Hα in HK		✓	✓		
2	Cβ–Hβ in γ hydroxy α–O–4′, β–5′ linked moieties (PC)	✓				
3	C–H in methoxyl	✓	✓	✓	✓	✓
4	Cγ–Hγ in α, and γ hydroxy β–O–4′ substructures	✓	✓	✓		✓
5	Cγ–Hγ in γ hydroxy substructures with double bond between α and β carbons (sinapyl or coniferyl alcohol)		✓	✓		
6	Cγ–Hγ in γ hydroxy β–O–4′, and α–O–4″ linked substructures	✓			✓	✓
7	Cγ–Hγ in γ hydroxy PC	✓	✓	✓	✓	
8	C–H in sugar residues	✓				
9	Cγ–Hγ in γ acylated β–O–4′ substructures	✓				
10, 11	Cγ–Hγ in α, and γ hydroxy β–O–4′ substructures		✓ ✓			
12	Cγ–Hγ in HK		✓	✓		
13	Cα–Hα in α hydroxy β–O–4′ substructures		✓	✓		
14	Cγ–Hγ in α–O–γ′, β–β′, and γ–O–α′ linked moieties (resinol)	✓	✓	✓	✓	✓
15	Cα–Hα in γ hydroxy β–O–4′, and α–O–4″ linked substructures				✓	
16	C–H in sugar residues	✓	✓	✓		
17	C–H in sugar residues	✓	✓	✓	✓	
18	C–H in sugar residues	✓				
19	C–H in sugar residues	✓			✓	
20	C–H in sugar residues		✓	✓	✓	
21			✓	✓		
22	C–H in sugar residues of phenyl glycoside type moieties		✓	✓		
23		✓				

their Cγ–Hγ correlations. Similarly, cross peaks are present for the Cγ–Hγ correlations in entities having β–O–4′ intermonomer linkages along with hydroxyl at α, and γ carbons. Of these, only the former is present in ESL3, indicating that α hydroxy β–O–4′ substructures are degraded, derivatized or mineralized at this treatment condition. On the other hand, ESL1, and ESL2 only have β–O–4′ substructures of the latter type as well as α hydroxy β–O–4′ moieties. In addition, SL also has β–O–4′ substructures with acylation at γ carbon. This molecular substructure is absent in all the ESLs indicating their mineralization with ET. It is interesting to note that the main β–O–4′ linked substructures in ESL4 are those with hydroxyl at α, and γ carbons with the α–O–4″ type entities showing only a subdued presence in the spectrum. ESL1 and ESL2 also have sinapyl alcohol or coniferyl alcohol end groups represented by their Cγ–Hγ correlations.

SL has resinol substructures – lignin monomer units simultaneously joined by α–O–γ′, β–β′, and γ–O–α′ linkages – represented by the Cγ–Hγ correlations. These substructures are retained during BL ET. SL also has phenylcoumaran (PC) substructures – entities with α–O–4′, β–5′ intermonomer linkages. It is observable by its Cβ–Hβ, and Cγ–Hγ correlations in the spectrum. These substructures withstand ET of BL and show their presence in the spectra of all the ESLs. The Cγ–Hγ correlations in the spectra are directly observed while the Cβ–Hβ cross peaks are overlapped by the strong methoxyl signals.

Two interesting cross peaks are observed in the spectra of ESL1, and ESL2 at 3.61–3.62/44.31–44.38 ppm, and 4.15–4.17/67.03–67.06 ppm, respectively. In technical literature, these peaks are correspondingly assigned to Cα–Hα, and Cγ–Hγ in Hibbert's ketone (HK) [17, 27]. These types of the substructures are reported to be formed during lignin depolymerization using acids [42, 48], but are not reported in soda and kraft lignins. ESL1 and ESL2, originating from SL through ET, are novel on this account. HK substructures in lignin can be subsequently converted to monomers with acetal functionality [42].

3.3.2 Aromatic and olefinic side chain

The attributed H–C correlations are tabulated in Table 5 [17, 41, 42, 45, 49–55]. SL has all the three types of – S, G and H – moieties in the macromolecule. C2,6–H2,6 correlations of S entities are well represented in the spectrum. Some of the S substructures are etherified at C4 while some have free phenolic hydroxyl. G moieties are represented by their prominent C5–H5 correlation. C2–H2 correlations are rather weak in the spectrum. Additionally, SL has H type enol ether (EE) substructures, confirmed through their Cα–Hα correlation. All the ESLs have S as well as G substructures. Barring ESL3, some of the S substructures are etherified at C4 and some are having free phenolic hydroxyl in other ESLs. The presence of HK substructures in ESL1 and ESL2 – lignins isolated after ET of BL at 11.11 mA/cm^2 – is further confirmed. These are both of S as well as G type in ESL1 but only G type in ESL2, suggesting demethoxylation with prolonged treatment. ESL3 and ESL4 are devoid of them. SL and all the ESLs have H type EE substructures, confirmed through their Cα–Hα correlation.

3.4 ^{1}H-NMR characterization and semi quantitative analysis

Fig. 2 (a) shows the ^{1}H-NMR spectrum for SL. The ^{1}H-NMR spectrum for the aromatic and olefinic region – 5 to 8 ppm – of SL is shown in Fig. 2 (b). Enlarged version of Fig. 2 and similar spectra for the ESLs are presented in the Supplement (Figs. S6 to S10). The main excitation regions for hydrogen attached to carbon are identified in correspondence with the ^{1}H–^{13}C HSQC NMR spectra and structural assignments are presented in Table 6.

3.4.1 Methoxyl groups abundance and distribution

Signal intensities in ^{1}H-NMR spectra are always quantitatively related to the type of hydrogen atoms. However, for a complex substance like lignin, there are too many closely spaced or overlapping signals difficult to precisely assign.

From Table 5 we observe that the H substructures in all the lignins are of EE type. The hydrogen attached to the olefinic α carbon in these moieties shows its signature frequency at 5.31–5.33 ppm in the ^{1}H-NMR spectra. This signal is distinctly located in the spectra, free from any crowding or overlapping. Therefore, the intensity of this signal can be used as a quantitative measure of the relative abundance of the H moieties. Taking advantage of this, the following procedure is used for the estimation of relative abundance of the S, G, and H substructures.

Let there be S the number of S units, G the number of G units, and H the number of H units in 100 phenylpropane units, so that:

$$S + G + H = 100. \tag{9}$$

Every S unit has two aromatic hydrogens, every G unit has three aromatic hydrogens, and every H unit has four aromatic hydrogens. Signal integration in the ^{1}H spectrum over 6.25–7.9 ppm range, therefore, is proportional to the sum of all aromatic hydrogen given by (2S + 3G + 4H). Each G unit has three methoxyl hydrogen, and each S unit has six methoxyl hydrogen. Integration of the methoxyl signal in ^{1}H spectrum, therefore, is proportional to the sum of all methoxyl hydrogen given by (6S + 3G). Therefore, we have:

$$\frac{6S + 3G}{2S + 3G + 4H} = \frac{I_{OMe}}{I_{Ar}}, \tag{10}$$

where I_{OMe} is the integral of the methoxyl signal and I_{Ar} is the integral over the aromatic region. Each EE type H

Table 5 ^{1}H–^{13}C HSQC NMR signal assignment to lignin molecular substructures and functionalities in 5–8/100–155 ppm region [17, 41, 42, 45, 49–55]

Signal identity in spectrum	Assignment	Presence of peaks				
		SL	ESL1	ESL2	ESL3	ESL4
24	C2,6–H2,6 in S moieties with ether linkage at C4	✓	✓	✓	✓	
25		✓	✓		✓	✓
26	C2,6–H2,6 in S moieties with free phenolic hydroxyl at C4	✓	✓	✓		✓
27	C2,6–H2,6 in S type HK		✓	✓		
28	C2–H2 in G moieties with free phenolic hydroxyl at C4. C2–H2 in ferulates		✓	✓		✓
29	C5–H5 in G type HK		✓			
30	C5–H5 in G moieties	✓	✓	✓	✓	✓
31	C6–H6 in G moieties				✓	
32	Cα–Hα in H type EE	✓	✓	✓	✓	✓
33					✓	
34	C6–H6 in ferulates		✓			

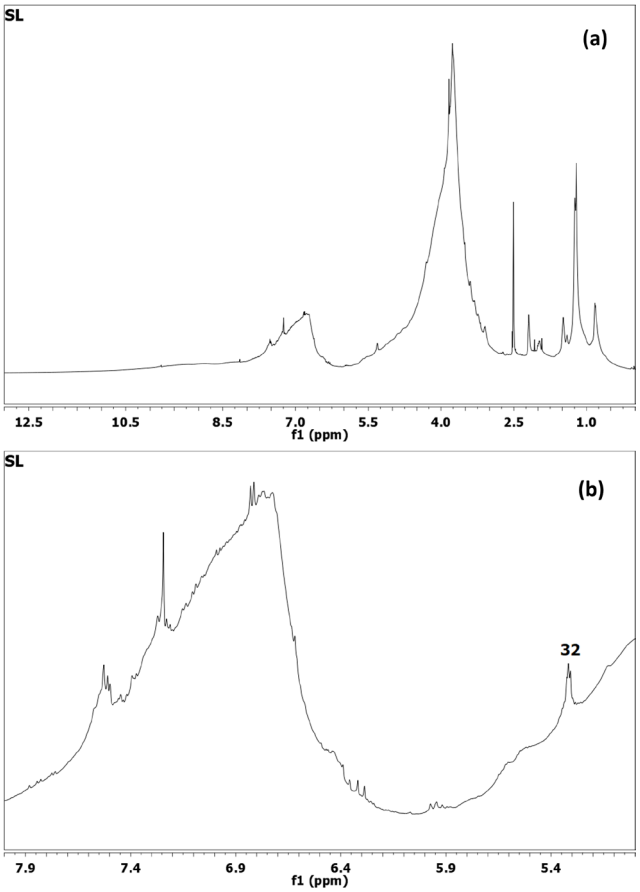


Fig. 2 [1]H-NMR spectrum of SL: (a) full spectrum; (b) aromatic region

unit has one hydrogen attached to the olefinic α carbon. Therefore, the integration of this signal is proportional to the sum of all such hydrogen given by H, so that:

$$\frac{\mathrm{H}}{2\mathrm{S}+3\mathrm{G}+4\mathrm{H}}=\frac{I_{\alpha\mathrm{H\ in\ EE}}}{I_{\mathrm{Ar}}}. \tag{11}$$

Here, $I_{\alpha\mathrm{H\ in\ EE}}$ is the integral of the signal for hydrogen attached to the olefinic α carbon. Solving the sets of Eqs. (9) to (11) for each lignin we get the values of S, G, and H.

The resulting values are shown in Table 7. It is evident that ET of BL results in significant overall demethoxylation at the aromatic ring. There is 8.7%–20% decrease in methoxyl in all the ESLs over that in SL. Beyond the overall decrease in methoxylthe ESLs have vastly altered S/G/H ratio. The S/G ratio drops by 46.3%–90.2% over that in SL. ESL3 has an appreciable rise in H content – more than double the proportion in SL – mostly at the cost of S content. Other ESLs get significantly richer in G content at the cost of S content. These lignins with lower S/G ratio, and ESL3 with higher H content, are expected to open new possibilities in polymerization and crosslinking applications in the domain of PF and epoxy resins and polyurethanes.

3.4.2 Aromatic acetyl groups abundance

All the lignin macromolecules have aliphatic as well as aromatic acetyl groups, as indicated from the HSQC spectra. However, the peaks corresponding to aliphatic acetyl groups, centered at 1.96–1.98 ppm, are not distinct in the [1]H-NMR spectra. But the aromatic acetyl groups are represented by clearly manifested peaks at 2.18–2.2 ppm. Signal integrations of these peaks provide the relative abundance of hydrogen in acetyl groups relative to hydrogen attached to the benzene ring measured as the ratio:

$$\frac{I_{\mathrm{Hydrogen\ in\ methyl\ of\ aromatic\ acetyl}}}{I_{\mathrm{Aromatic\ hydrogen}}}. \tag{12}$$

As shown in Table 4, All the ESLs, except ESL2, are more acetylated than SL in the aromatic ring. ESL3 is the most acetylated in the aromatic ring followed by ESL4. Extent of acetylation in ESL2 is comparable to that of SL. Lower CD and SC tend to increase the acetylation on the aromatic ring.

Table 6 [1]H-NMR assignment to main lignin molecular substructures and functionalities

Peak / region (ppm)	SL	ESL1	ESL2	ESL3	ESL4	Assignment
1.98–2.05	✓	✓	✓	✓	✓	Aliphatic acetyl hydrogen
2.18–2.2	✓	✓	✓	✓	✓	Aromatic acetyl hydrogen
3.01–3.64	✓	✓	✓	✓	✓	Hydrogen in aliphatic side chain
3.73–3.84	✓	✓	✓	✓	✓	Hydrogen in methoxyl
3.91	✓					Hγ in γ acylated β–O–4′ moieties
4.11–4.88	✓	✓	✓	✓		Hydrogen in aliphatic side chain
5.31–5.33	✓	✓	✓	✓	✓	Hα in EE
6.25–7.9	✓	✓	✓	✓	✓	Hydrogen attached to aromatic ring
3.09–4.3	✓	✓	✓	✓		Hydrogen in sugar residue
9.62–9.78		✓	✓			Hydrogen in hydroxyl of carboxylic acid

Table 7 ^{1}H-NMR quantitative assessment of methoxyl and aromatic acetyl in lignins

Moiety	SL	ESL1	ESL2	ESL3	ESL4
S (%)	26.76 ± 0.29	16.79 ± 0.15	9.66 ± 0.10	18 ± 0.20	3.59 ± 0.04
G (%)	64.79 ± 0.60	74.45 ± 0.71	84.38 ± 0.85	64 ± 0.61	87.43 ± 0.88
H (%)	8.45 ± 0.08	8.76 ± 0.09	5.96 ± 0.06	18 ± 0.17	8.98 ± 0.09
Methoxyl group / 100 aromatic ring	118.31	108.03	103.7	100	94.61
S/G	0.41	0.22	0.11	0.28	0.04
S/G/H	3.17/7.67/1	1.92/8.50/1	1.62/14.16/1	1/3.55/1	0.40/9.74/1
Aromatic acetyl (hydrogen/aromatic hydrogen)	0.06 ± 0.001	0.09 ± 0.001	0.07 ± 0.001	0.15 ± 0.002	0.11 ± 0.002

3.4.3 Carboxylic acid groups

ESL1 and ESL2 have proton signals for hydroxyl in carboxylic acid group showing at 9.62–9.63, and 9.77–9.78 ppm in the ^{1}H-NMR spectra. In no other lignin such signals are present. It appears that free carboxylic acid groups are produced only at a high CD of 11.11 ± 0.02 mA/cm^2. Based on the discussion in Sections 3.3.1, 3.3.2, and 3.4.3 a summary of different structural features in SL and ESLs is presented in Table 8.

3.5 Thermochemical characterization

Fig. 3 shows the TGA and DTG plots of the lignins. Enlarged version of Fig. 3 is available in the Supplement (Fig. S11). SL shows the usual nature of soda lignin. Main thermal decomposition spans from about 200 to 470 °C, accounting for 55% mass loss. Maximum mass loss rate of 20.26 ± 0.18 mass%/min occurs at temperature T_{max} of 385.7±2.2 °C. It leaves a char residue of 24.9 ± 0.20% (22.08 ± 0.28% corrected for ash) at 850 °C. The nature of the thermal decomposition of ESL1 is similar to SL, but at a slower rate, and the onset appears somehow earlier at about 175 °C. 42% mass loss is observed in the main thermal decomposition temperature window of about 175 to 480 °C. T_{max} for ESL1 is 374 ± 2.4 °C with the maximum rate of mass loss being 14.2 ± 0.13 mass%/min. The residual char is 38.2 ± 0.29% (35.44 ± 0.36% corrected for ash) at 850 °C. ESL2 is the slowest to thermally decompose, the main decomposition occurring between about 165 to 420 °C that causes 26.9% mass loss. T_{max} is further lowered to 370 ± 3.5 °C with 8.7 ± 0.07 mass%/min maximum rate of mass loss. 46.0 ± 0.43% (42.89 ± 0.53% corrected for ash) char is obtained at 850 °C, which is almost double the amount obtained from SL. This quantity is also the highest among all the ESLs. ESL2 also shows a brief second stage of thermal decomposition between about 470 and 490 °C. One can also notice the onset of a third thermal degradation stage nearly at 795 °C. ESL3 is the most unusual in its thermal degradation behavior. Onset of the main thermal degradation appears at about 165 °C and continues to nearly 425 °C. 31.7% mass is lost in this range. Maximum rate of mass loss of 9.4 ± 0.1 mass%/min occurs at 355 ± 3.3 °C. The distinct feature of this lignin is a pronounced and extended second stage of thermal degradation that starts nearly at 470 °C and continues till about 655 °C. The second stage accounts for 23.65% mass loss, with the degradation rate peaking to 7.6 ± 0.08 mass%/min

Table 8 Major structural features in SL and ESLs

Structural feature	SL	ESL1	ESL2	ESL3	ESL4
β–O–4′ plus α–O–4″	✓			✓	✓
α, and *γ* hudroxy *β*–O–4′	✓	✓	✓		✓
α hydroxy *β*–O–4′		✓	✓		
γ acylated *β*–O–4′	✓				
Sinapyl or coniferyl alcohol end group		✓	✓		
Resinol	✓	✓	✓	✓	✓
PC	✓	✓	✓	✓	✓
HK		✓	✓		
S	✓	✓	✓	✓	✓
G	✓	✓	✓	✓	✓
H type EE	✓	✓	✓	✓	✓
Carboxylic acid		✓	✓		

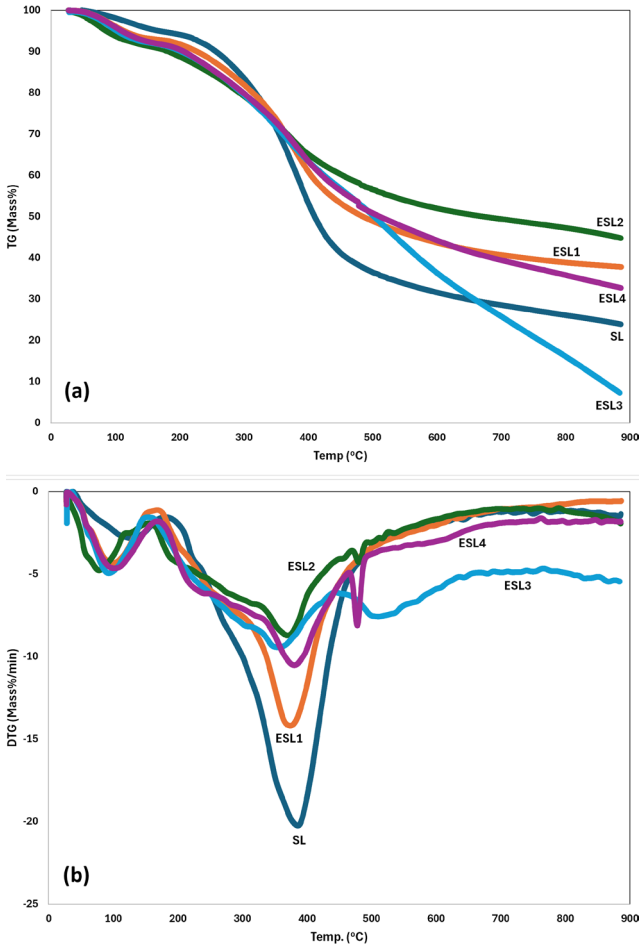


Fig. 3 TG and DTG plots of different lignins: (a) TG; (b) DTG

at 510 ± 4.9 °C. Even the onset of a third stage of decomposition is observed near 785 °C, and the material continues to lose mass at a noticeable rate and leaves only 10.9 ± 0.1% (8.11 ± 0.18% corrected for ash) char residue at 850 °C. The main thermal decomposition of ESL4 is observed between about 180 °C and 455 °C with a broad shoulder in DTG appearing between 220 and 330 °C. Mass loss during the main thermal decomposition is 35.8%. T_{max} is 380 ± 3.6 °C and the maximum rate of mass loss 10.5 ± 0.1 mass%/min. A brief second stage of thermal decomposition is observed between about 470 and 490 °C. ESL4 leaves 34.0 ± 0.4% (30.95 ± 0.49% corrected for ash) char at 850 °C. Overall, we find that all the ESLs are thermally more stable than SL up to 625 °C. Increased thermal stability – more residual char and lower rate of degradation – is a much sought after feature in many polymer and polymer composite applications. On this account, ESLs may be better suited than SL in applications where resistance to thermal degradation and fire retardance are important.

4 Conclusion

ET of BL prior to lignin separation by acidification can significantly affect the yield and macromolecular structure of the resulting lignin. Lower CD and higher SC has a lowering effect on lignin yield after acidification. ET of BL causes demethoxylation; the effect being more pronounced at lower CD and higher SC. Resulting lignins have significantly reduced S/G ratios. This is also associated with a corresponding increase in the phenolic hydroxyl content of ESLs, increasing with lower CD and higher SC. *β*–*β*′ linked resinol moieties are completely degraded at high CD but partially survives treatment at low CD. *β*–5′ linked PC, the other type of condensed substructure, survives ET except for treatment at low CD and high SC. High CD also introduces HK type moieties in the lignin macromolecule. Moreover, ET increases lignin acetylation at the aromatic ring. Except ESL3, all the ESLs are thermally more stable than SL and ends with appreciably higher char. Once started, ESL3 slowly but steadily degrades over almost the entire temperature range and leaves only a minimal amount of char at 850 °C. Even this lignin is thermally more stable than SL up to 625 °C.

References

[1] Mastrolitti, S., Borsella, E., Giuliano, A., Petrone, M. T., De Bari, I., Gosselink, R., van Erven, G., Annevelink, E., Triantafyllidis, K. S., Stichnothe, H. "Sustainable lignin valorization: Technical lignin, processes and market development", IEA Bioenergy, 2021. ISBN 979-12-80907-01-1 [online] Available at: https://task42.ieabioenergy.com/wp-content/uploads/sites/10/2021/11/Sustainable-Lignin-Valorization_rev26-01-2022.pdf [Accessed: 25 May 2026]

[2] Ghatak, H. R. "Lignin: Isolation, Characterization, and Value Addition", CRC Press, 2025. ISBN 9781003598664 https://doi.org/10.1201/9781003598664

[3] Argyropoulos, D. D. S., Crestini, C., Dahlstrand, C., Furusjö, E., Gioia, C., …, Wimby, M. "Kraft Lignin: A Valuable, Sustainable Resource, Opportunities and Challenges", ChemSusChem, 16(23), e202300492, 2023. https://doi.org/10.1002/cssc.202300492

[4] Lu, X., Zhu, X., Dai, P., Robin, H. M., Guo, H., …, Gu, X. "Thermal performance and thermal decomposition kinetics of a novel lignin-based epoxy resin containing phosphorus and nitrogen elements", Journal of Thermal Analysis and Calorimetry, 147(8), pp. 5237–5253, 2022. https://doi.org/10.1007/s10973-021-10950-9

[5] Gondaliya, A., Nejad, M. "Lignin as a Partial Polyol Replacement in Polyurethane Flexible Foam", Molecules, 26(8), 2302, 2021. https://doi.org/10.3390/molecules26082302

[6] Zhang, N., Li, Z., Xiao, Y., Pan, Z., Jia, P., Feng, G., Bao, C., Zhou, Y., Hua, L. "Lignin-based phenolic resin modified with whisker silicon and its application", Journal of Bioresources and Bioproducts, 5(1), pp. 67–77, 2020. https://doi.org/10.1016/j.jobab.2020.03.008

[7] Arnawtee, W. H., Jaleh, B., Nasrollahzadeh, M., Bakhshali-Dehkordi, R., Nasri, A., Orooji, Y. "Lignin valorization: Facile synthesis, characterization and catalytic activity of multiwalled carbon nanotubes/kraft lignin/Pd nanocomposite for environmental remediation", Separation and Purification Technology, 290, 120793, 2022. https://doi.org/10.1016/j.seppur.2022.120793

[8] Bai, J., Wang, S., Li, Y., Wang, Z., Tang, J. "Effect of chemical structure and molecular weight on the properties of lignin-based ultrafine carbon fibers", International Journal of Biological Macromolecules, 187, pp. 594–602, 2021. https://doi.org/10.1016/j.ijbiomac.2021.07.149

[9] Enengl, C., Lumetzberger, A., Duchoslav, J., Mardare, C. C., Ploszczanski, L., Rennhofer, H., Unterweger, C., Stifter, D., Fürst, C. "Influence of the carbonization temperature on the properties of carbon fibers based on technical softwood kraft lignin blends", Carbon Trends, 5, 100094, 2021. https://doi.org/10.1016/j.cartre.2021.100094

[10] Conde, J. J., González-Rodríguez, S., Chen, X., Lu-Chau, T. A., Eibes, G., Pizzi, A., Moreira, M. T. "Electrochemical oxidation of lignin for the simultaneous production of bioadhesive precursors and value-added chemicals", Biomass and Bioenergy, 169, 106693, 2023. https://doi.org/10.1016/j.biombioe.2022.106693

[11] Singh, S., Ghatak, H. R. "Vanillin Formation by Electrooxidation of Lignin on Stainless Steel Anode: Kinetics and By-Products", Journal of Wood Chemistry and Technology, 37(6), pp. 407–422, 2017. https://doi.org/10.1080/02773813.2017.1310899

[12] Singh, S., Ghatak, H. R. "Process optimization of lignin conversion into value added chemicals by thermochemical pretreatment and electrooxidation on a stainless steel anode", Holzforschung, 72(3), pp. 187–199, 2018. https://doi.org/10.1515/hf-2017-0108

[13] Chen, S., Cheng, H., Wu, S. "Pyrolysis characteristics and volatiles formation rule of organic solvent fractionized kraft lignin", Fuel, 270, 117520, 2020. https://doi.org/10.1016/j.fuel.2020.117520

[14] Lauwaert, J., Stals, I., Lancefield, C. S., Deschaumes, W., Depuydt, D., Vanlerberghe, B., Devlamynck, T., Bruijnincx, P. C. A., Verberckmoes, A. "Pilot scale recovery of lignin from black liquor and advanced characterization of the final product", Separation and Purification Technology, 221, pp. 226–235, 2019. https://doi.org/10.1016/j.seppur.2019.03.081

[15] Sheng, Y., Ma, Z., Wang, X., Han, Y. "Ethanol organosolv lignin from different agricultural residues: Toward basic structural units and antioxidant activity", Food Chemistry, 376, 131895, 2022. https://doi.org/10.1016/j.foodchem.2021.131895

[16] Serrano, L., Esakkimuthu, E. S., Marlin, N., Brochier-Salon, M.-C., Mortha, G., Bertaud, F. "Fast, Easy, and Economical Quantification of Lignin Phenolic Hydroxyl Groups: Comparison with Classical Techniques", Energy & Fuels, 32(5), pp. 5969–5977, 2018. https://doi.org/10.1021/acs.energyfuels.8b00383

[17] Paulsen Thoresen, P., Lange, H., Crestini, C., Rova, U., Matsakas, L., Christakopoulos, P. "Characterization of Organosolv Birch Lignins: Toward Application-Specific Lignin Production", ACS Omega, 6(6), pp. 4374–4385, 2021. https://doi.org/10.1021/acsomega.0c05719

[18] El Mansouri, N.-E., Yuan, Q., Huang, F. "Synthesis and characterization of kraft lignin-based epoxy resins", BioResources, 6(3), pp. 2492–2503, 2011. [online] Available at: https://bioresources.cnr.ncsu.edu/resources/synthesis-and-characterization-of-kraft-lignin-based-epoxy-resins/ [Accessed: 25 May 2026]

[19] Malutan, T., Nicu, R., Popa, V. I. "Lignin modification by epoxidation", BioResources, 3(4), pp. 1371–1376, 2008. [online] Available at: https://bioresources.cnr.ncsu.edu/BioRes_03/BioRes_03_4_1371_Malutan_NP_Lignin_Mod_Epoxidation_278.pdf [Accessed: 25 May 2026]

[20] Ott, M. W., Dietz, C., Trosien, S., Mehlhase, S., Bitsch, M. J.,…, Biesalski, M. "Co-curing of epoxy resins with aminated lignins: insights into the role of lignin homo crosslinking during lignin amination on the elastic properties", Holzforschung, 75(4), pp. 390–398. 2021. https://doi.org/10.1515/hf-2020-0060

[21] Li, J., Zhang, J., Zhang, S., Gao, Q., Li, J., Zhang, W. "Fast Curing Bio-Based Phenolic Resins via Lignin Demethylated under Mild Reaction Condition", Polymers, 9(9), 428, 2017. https://doi.org/10.3390/polym9090428

[22] Konduri, M. K., Kong, F., Fatehi, P. "Production of carboxymethylated lignin and its application as a dispersant", European Polymer Journal, 70, pp. 371–383, 2015. https://doi.org/10.1016/j.eurpolymj.2015.07.028

[23] Benar, P., Gonçalves, A. R., Mandelli, D., Schuchardt, U. "Eucalyptus organosolv lignins: study of the hydroxymethylation and use in resols", Bioresource Technology, 68(1), pp. 11–16, 1999. https://doi.org/10.1016/S0960-8524(98)00076-5

[24] Pinheiro, F. G. C., Soares, A. K. L., Santaella, S. T., Silva, L. M. A., Canuto, K. M., Cáceres, C. A., Rosa, M. d. F., Feitosa, J. P. d. A., Leitão, R. C. "Optimization of the acetosolv extraction of lignin from sugarcane bagasse for phenolic resin production", Industrial Crops and Products, 96, pp. 80–90, 2017. https://doi.org/10.1016/j.indcrop.2016.11.029

[25] Cateto, C. A., Barreiro, M. F., Rodrigues, A. E. "Monitoring of lignin-based polyurethane synthesis by FTIR-ATR", Industrial Crops and Products, 27(2), pp. 168–174, 2008. https://doi.org/10.1016/j.indcrop.2007.07.018

[26] Cateto, C. A., Barreiro, M. F., Rodrigues, A. E., Belgacem, M. N. "Kinetic study of the formation of lignin-based polyurethanes in bulk", Reactive and Functional Polymers, 71(8), pp. 863–869, 2011. https://doi.org/10.1016/j.reactfunctpolym.2011.05.007

[27] Antonino, L. D., Gouveia, J. R., de Sousa Júnior, R. R., Garcia, G. E. S., Gobbo, L. C., Tavares, L. B., dos Santos, D. J. "Reactivity of Aliphatic and Phenolic Hydroxyl Groups in Kraft Lignin towards 4,4′ MDI", Molecules, 26(8), 2131, 2021. https://doi.org/10.3390/molecules26082131

[28] Cateto, C. A., Barreiro, M. F., Rodrigues, A. E., Belgacem, M. N. "Optimization Study of Lignin Oxypropylation in View of the Preparation of Polyurethane Rigid Foams", Industrial & Engineering Chemistry Research, 48(5), pp. 2583–2589, 2009. https://doi.org/10.1021/ie801251r

[29] Gouveia, J. R., Garcia, G. E. S., Antonino, L. D., Tavares, L. B., dos Santos, D. J. "Epoxidation of Kraft Lignin as a Tool for Improving the Mechanical Properties of Epoxy Adhesive", Molecules, 25(11), 2513, 2020. https://doi.org/10.3390/molecules25112513

[30] Nikafshar, S., Wang, J., Dunne, K., Sangthonganotai, P., Nejad, M. "Choosing the Right Lignin to Fully Replace Bisphenol A in Epoxy Resin Formulation", ChemSusChem, 14(4), pp. 1184–1195, 2021. https://doi.org/10.1002/cssc.202002729

[31] Gioia, C., Colonna, M., Tagami, A., Medina, L., Sevastyanova, O., Berglund, L. A., Lawoko, M. "Lignin-Based Epoxy Resins: Unravelling the Relationship between Structure and Material Properties", Biomacromolecules, 21(5), pp. 1920–1928, 2020. https://doi.org/10.1021/acs.biomac.0c00057

[32] Singh, S., Ghatak, H. R. "Optimal Synthesis of Aromatic Carbonyl Compounds by Electrooxidation of Soda Lignins on Stainless steel and TiMMO Anodes", Iranian Journal of Chemistry and Chemical Engineering, 40(6), pp. 1814–1839, 2021. https://doi.org/10.30492/ijcce.2020.43449

[33] Schmitt, D., Regenbrecht, C., Hartmer, M., Stecker, F., Waldvogel, S. R. "Highly selective generation of vanillin by anodic degradation of lignin: a combined approach of electrochemistry and product isolation by adsorption", Beilstein Journal of Organic Chemistry, 11, pp. 473–480, 2015. https://doi.org/10.3762/bjoc.11.53

[34] Stiefel, S., Schmitz, A., Peters, J., Di Marino, D., Wessling, M. "An integrated electrochemical process to convert lignin to value-added products under mild conditions", Green Chemistry, 18(18), pp. 4999–5007, 2016. https://doi.org/10.1039/c6gc00878j

[35] BIS "IS 6911:2017 Stainless steel plate, sheet and strip - Specification (Second Revision)", Bureau of Indian Standards, New Delhi, India, 2017.

[36] Mestrelab Research "MestReNova, (6.0.2.5475)", [computer program] Available at: https://mestrelab.com [Accessed: 17 July 2009]

[37] Ghatak, H. R. "Advanced Oxidation Processes for the Treatment of Biorecalcitrant Organics in Wastewater", Critical Reviews in Environmental Science and Technology, 44(11), pp. 1167–1219, 2014. https://doi.org/10.1080/10643389.2013.763581

[38] Hayyan, M., Hashim, M. A., AlNashef, I. M. "Superoxide Ion: Generation and Chemical Implications", Chemical Reviews, 116(5), pp. 3029–3085, 2016. https://doi.org/10.1021/acs.chemrev.5b00407

[39] Luo, Z., Yan, Y., Spinney, R., Dionysiou, D. D., Villamena, F. A., Xiao, R., Vione, D. "Environmental implications of superoxide radicals: From natural processes to engineering applications", Water Research, 261, 122023, 2024. https://doi.org/10.1016/j.watres.2024.122023

[40] Meena, V. K., Ghatak, H. R. "Electrochemical Advanced Oxidation of Lamotrigine at Ti/DSA (Ta_2O_5-Ir_2O_5) and Stainless Steel Anodes", Journal of Electrochemical Science and Technology, 13(2), pp. 292–307, 2022. https://doi.org/10.33961/jecst.2021.01074

[41] Audu, I. G., Brosse, N., Winter, H., Hoffmann, A., Bremer, M., Fischer, S., Laborie, M.-P. "Acetyl Groups in *Typha capensis*: Fate of Acetates during Organosolv and Ionosolv Pulping", Polymers, 10(6), 619, 2018. https://doi.org/10.3390/polym10060619

[42] Miles-Barrett, D. M., Neal, A. R., Hand, C., Montgomery, J. R. D., Panovic, I., Ojo, O. S., Lancefield, C. S., Cordes, D. B., Slawin, A. M. Z., Lebl, T., Westwood, N. J. "The synthesis and analysis of lignin-bound Hibbert ketone structures in technical lignins", Organic & Biomolecular Chemistry, 14(42), pp. 10023–10030, 2016. https://doi.org/10.1039/C6OB01915C

[43] Rencoret, J., Ralph, J., Marques, G., Gutiérrez, A., Martínez, Á. T., del Río, J. C. "Structural Characterization of Lignin Isolated from Coconut (*Cocos nucifera*) Coir Fibers", Journal of Agricultural and Food Chemistry, 61(10), pp. 2434–2445, 2013. https://doi.org/10.1021/jf304686x

[44] Tan, X., Jiang, B., Yang, Y., Min, D., Jin, Y. "Structural characteristics of milled wood lignin (MWL) isolated from green liquor (GL) pretreated poplar (*Populus deltoides*)", Holzforschung, 71(2), pp. 99–108, 2017. https://doi.org/10.1515/hf-2016-0093

[45] Wen, J.-L., Sun, S.-L., Xue, B.-L., Sun, R.-C. "Recent Advances in Characterization of Lignin Polymer by Solution-State Nuclear Magnetic Resonance (NMR) Methodology", Materials, 6(1), pp. 359–391, 2013. https://doi.org/10.3390/ma6010359

[46] Yáñez-S, M., Matsuhiro, B., Nuñez, C., Pan, S., Hubbell, C. A., Sannigrahi, P., Ragauskas, A. J. "Physicochemical characterization of ethanol organosolv lignin (EOL) from *Eucalyptus globulus*: Effect of extraction conditions on the molecular structure", Polymer Degradation and Stability, 110, pp. 184–194, 2014. https://doi.org/10.1016/j.polymdegradstab.2014.08.026

[47] You, T.-T., Zhang, L.-M., Zhou, S.-K., Xu, F. "Structural elucidation of lignin–carbohydrate complex (LCC) preparations and lignin from *Arundo donax* Linn", Industrial Crops and Products, 71, pp. 65–74, 2015. https://doi.org/10.1016/j.indcrop.2015.03.070

[48] Wang, S., Li, H., Xiao, L.-P., Song, G. "Unraveling the Structural Transformation of Wood Lignin During Deep Eutectic Solvent Treatment", Frontiers in Energy Research, 8, 48, 2020. https://doi.org/10.3389/fenrg.2020.00048

[49] Yuan, T.-Q., Sun, S.-N., Xu, F., Sun, R.-C. "Characterization of Lignin Structures and Lignin–Carbohydrate Complex (LCC) Linkages by Quantitative ^{13}C and 2D HSQC NMR Spectroscopy", Journal of Agricultural and Food Chemistry, 59(19), pp. 10604–10614, 2011. https://doi.org/10.1021/jf2031549

[50] Constant, S., Wienk, H. L. J., Frissen, A. E., Peinder, P. d., Boelens, R., …, Bruijnincx, P. C. A. "New insights into the structure and composition of technical lignins: a comparative characterisation study", Green Chemistry, 18(9), pp. 2651–2665, 2016. https://doi.org/10.1039/c5gc03043a

[51] del Río, J. C., Rencoret, J., Prinsen, P., Martinez, Á. T., Ralph, J., Gutiérrez, A. "Structural Characterization of Wheat Straw Lignin as Revealed by Analytical Pyrolysis, 2D-NMR, and Reductive Cleavage Methods", Journal of Agricultural and Food Chemistry, 60(23), pp. 5922–5935, 2012. https://doi.org/10.1021/jf301002n

[52] Li, M.-F., Sun, S.-N., Xu, F., Sun, R.-C. "Formic acid based organosolv pulping of bamboo (*Phyllostachys acuta*): Comparative characterization of the dissolved lignins with milled wood lignin", Chemical Engineering Journal, 179, pp. 80–89, 2012. https://doi.org/10.1016/j.cej.2011.10.060

[53] Moniz, P. Serralheiro, C., Matos, C. T., Boeriu, C. G., Frissen, A. E., Duarte, L. C., Roseiro, L. B., Pereira, H., Carvalheiro, F. "Membrane separation and characterisation of lignin and its derived products obtained by a mild ethanol organosolv treatment of rice straw", Process Biochemistry, 65, pp. 136–145, 2018. https://doi.org/10.1016/j.procbio.2017.11.012

[54] Shi, Z., Xu, G., Deng, J., Dong, M., Murugadoss, V., Liu, C., Shao, Q., Wu, S., Guo, Z. "Structural characterization of lignin from *D. sinicus* by FTIR and NMR techniques", Green Chemistry Letters and Reviews, 12(3), pp. 235–243, 2019. https://doi.org/10.1080/17518253.2019.1627428

[55] Schlee, P., Tarasov, D., Rigo, D., Balakshin, M. "Advanced NMR Characterization of Aquasolv Omni (AqSO) Biorefinery Lignins/Lignin-Carbohydrate Complexes", ChemSusChem, 16(18), e202300549, 2023. https://doi.org/10.1002/cssc.202300549